

SINTERED METALS AND ALLOYS

BEHAVIOR OF EUTECTIC Ti–Si–Zr TITANIUM ALLOYS IN DIFFERENT FRICTION CONDITIONS

I.D. Gorna,^{1,3} K.E. Grinkevich,¹ K.O. Valuyskaya,¹ I.V. Tkachenko,¹
V.T. Varchenko,¹ V.M. Novichenko,² V.V. Kremenitsky,²
and S.O. Firstov¹

UDC 669.295:620.17

The tribological properties of heterogeneous Ti–Si–Zr titanium alloys with an $e(\beta\text{-Ti} + (\text{Ti}, \text{Zr})_2\text{Si})$ eutectic were studied in different friction conditions. Tribological tests were performed with two methods. The samples were subjected to shaft–bush (counterface–material) tests by dry friction against ShKh15 steel employing an M-22M machine at a load of 20 N and a sliding speed of 1–6 m/sec with one method. The other method involved quasistatic and dynamic sphere–plane tests with an effective load of 30 N employing a computer-assisted tribology system. The indenter materials were ShKh15 steel and Si_3N_4 ceramics. The tests were performed at a sliding speed of approximately 0.0147 m/sec in water. The linear and weight wear rate for the cast Ti–10Si–10Zr–1Sn sample with a superfine eutectic structure determined with the first method at the greatest test speed (6 m/sec) was found to be 1.4 times higher than that of the Ti–9Si–7.6Zr alloy. The Ti–10Si–10Zr–1Sn alloy showed the lowest wear resistance under quasistatic and dynamic loads with the second method, regardless of the indenter material (ShKh15 or Si_3N_4). Contrastingly to the previous data for cast irons and steels, the eutectic Ti–Si–Zr titanium alloys for the first time showed smaller wear under dynamic loading than under quasistatic loading. Thermomechanical treatment of the hypoeutectic Ti–9Si–7.6Zr alloy was established to increase its wear resistance by more than 1.6 times.

Keywords: eutectic Ti–Si–Zr titanium alloys, tribotechnical properties, quasistatic and dynamic wear.

INTRODUCTION

Titanium alloys are finding increased application in various industries as structural materials. In addition, titanium-based alloys are currently used in biotribology, where the influence of different loading methods (quasistatic and dynamic) on friction processes is very important. Nevertheless, their applications are known to be significantly limited by low wear resistance caused by the tendency to contact seizure and, as a consequence, significant wear and mechanical damage to the contacting surfaces [1–3].

¹Frantsevich Institute for Problems of Materials Science, National Academy of Sciences of Ukraine, Kyiv, Ukraine. ²Technical Center, National Academy of Sciences of Ukraine, Kyiv, Ukraine.

³To whom correspondence should be addressed; e-mail: igornaya@gmail.com.

Translated from Poroshkova Metallurgiya, Vol. 61, Nos. 7–8 (546), pp. 56–66, 2022. Original article submitted May 7, 2022.

Should titanium alloys be used in tribotechnical units, heat (thermochemical) treatment or coating deposition can significantly decrease the friction losses and increase the wear resistance of parts [4–9].

An alternative method to increase the tribotechnical properties of titanium alloys is to develop structures that should be substantially heterogeneous and consist of hard grains distributed in an elastoplastic metal matrix [10, 11]. Such materials include metal-matrix composites representing a strengthening precipitate phase and a metal matrix. According to their mechanical properties, these materials are intermediate between metal and ceramic materials and combine high hardness, wear resistance, and ductility. Materials with such structures, including coatings, are commonly produced by powder metallurgy methods.

The so-called natural (*in situ*) composites, resulting from the crystallization of eutectic alloys under conventional casting, have a heterogeneous structure as well [12, 13]. Note that the reliable operation of wear-resistant materials requires strong adhesive bonding between the hard inclusions and the matrix, which is peculiar to eutectic alloys [12, 13].

In situ composites in the binary Ti–Si system, the so-called ‘titanium pigs’ [14], generally meet the above requirements: α -Ti (β^* -Ti) is the matrix and Ti_5Si_3 is the strengthening phase in such alloys [14–16]. The papers [17–19] reported that additional doping of binary Ti–Si alloys with zirconium allowed their phase composition and the mechanical properties of respective phases to be changed. Thus, when more than 10 at.% (5 wt.%) Zr is introduced, a ternary intermetallic (Ti, Zr)₂Si phase is formed instead of Ti_5Si_3 . This phase significantly differs from Ti_5Si_3 both in the morphology and size and in the properties [17–20].

Note that the antifriction properties of eutectic titanium alloys have not been extensively studied [21–23]. The paper [21] examined the tribological properties of Ti–Si–Zr alloys with 2–10 at.% Si and 2.6 at.% Zr and established that the antifriction properties of the Ti–10 at.% Si–2.6 at.% Zr alloy with an $\epsilon(\beta^*\text{-Ti} + Ti_5Si_3)$ eutectic were more than five times greater than those of the commercial Ti–6Al–4V alloy. The papers [22, 23] show that additional doping (Al, Ga) of the eutectic Ti–Si alloys can significantly improve their wear resistance.

The objective is to examine the tribotechnical properties of eutectic Ti–Si–Zr alloys with increased zirconium content and to evaluate and compare their behavior in different friction conditions.

EXPERIMENTAL PROCEDURE

Two titanium alloys were examined, Ti–10Si–10Zr–1Sn and Ti–9Si–7.6Zr (Table 1), whose structure and mechanical properties were studied in [18, 20]. The Ti–10Si–10Zr–1Sn alloy friction samples were made of a cast 100 g ingot produced by arc melting with a nonconsumable tungsten electrode on a water-cooled copper hearth in an argon atmosphere additionally purified with a molten titanium getter. The starting materials were iodide-refined titanium and zirconium (99.97%), tin (99.99%), and silicon (commercially pure).

The Ti–9Si–7.6Zr alloy samples were made from an ingot weighing ~5 kg produced by argon-arc melting and were examined in as-cast state and after thermomechanical treatment such as rolling at 1000°C to 66% reduction. The starting materials were VT-0 titanium, zirconium (99.97%), and silicon (commercially pure).

Tribological tests were performed using two methods under different friction conditions [24–26]. In one method, the samples were subjected to shaft–bush (counterface–material) wear tests by dry friction employing an

TABLE 1. Chemical and Phase Compositions, Vickers Hardness, and Elastic Modulus of Eutectic Ti–Si–Zr Alloys [18, 20]

Chemical composition, at.%	Phase composition	HV30, GPa	E, GPa
Ti–10Si–10Zr–1Sn (cast)	α -Ti + (Ti, Zr) ₂ Si + $Ti_5Si_3^*$	3.6	137
Ti–9Si–7.6Zr (cast)	α -Ti + (Ti, Zr) ₂ Si + $Ti_5Si_3^*$	3.9	128
Ti–9Si–7.6Zr (treated thermomechanically)	α -Ti + (Ti, Zr) ₂ Si + $Ti_5Si_3^*$	4.0	134

* Ti_5Si_3 traces.

M-22M machine at $N = 20$ N and sliding speeds of 1, 2, 4, and 6 m/sec in normal conditions. The friction path was 3 km for each speed. The samples were tested by friction against ShKh15 steel with HRC 61–63 hardness and $R_a = 0.32$ – 0.63 roughness [24].

The other method included sphere–plane tests employing a computer-assisted tribology system equipped with a dynamic load module [25, 26]. Quasistatic or dynamic effective loads of 30 N acted on a spherical steel (ShKh15) or ceramic (Si_3N_4) indenter with a diameter of 8 mm that was reciprocally sliding over a plane sample. The experiments were performed in distilled water at a sliding speed of ~ 0.0147 m/sec, friction length of ~ 1200 sec, and friction path of ~ 17.64 m. Linear wear was determined with a Kalibr K-201 surface recorder/analyzer [25]. The friction force was indicated on the tribological patterns plotted with the self-recorder.

The structure of friction paths was examined employing a Jenaphot-2000 optical microscope.

RESULTS AND DISCUSSION

According to [18], the cast Ti–10Si–10Zr–1Sn alloy has a superfine heterogeneous structure with an $\epsilon(\beta^*\text{-Ti} + (\text{Ti}, \text{Zr})_2\text{Si})$ eutectic (Fig. 1*a, b*) and approximately 50 vol.% $(\text{Ti}, \text{Zr})_2\text{Si}$.

Contrastingly to the Ti–10Si–10Zr–1Sn alloy, the cast Ti–9Si–7.6Zr alloy has a hypoeutectic structure with an α -Ti matrix and an $\epsilon(\beta^*\text{-Ti} + (\text{Ti}, \text{Zr})_2\text{Si})$ eutectic (Fig. 1*c, d*; Table 1) [20]. Figure 1*d* shows a TEM

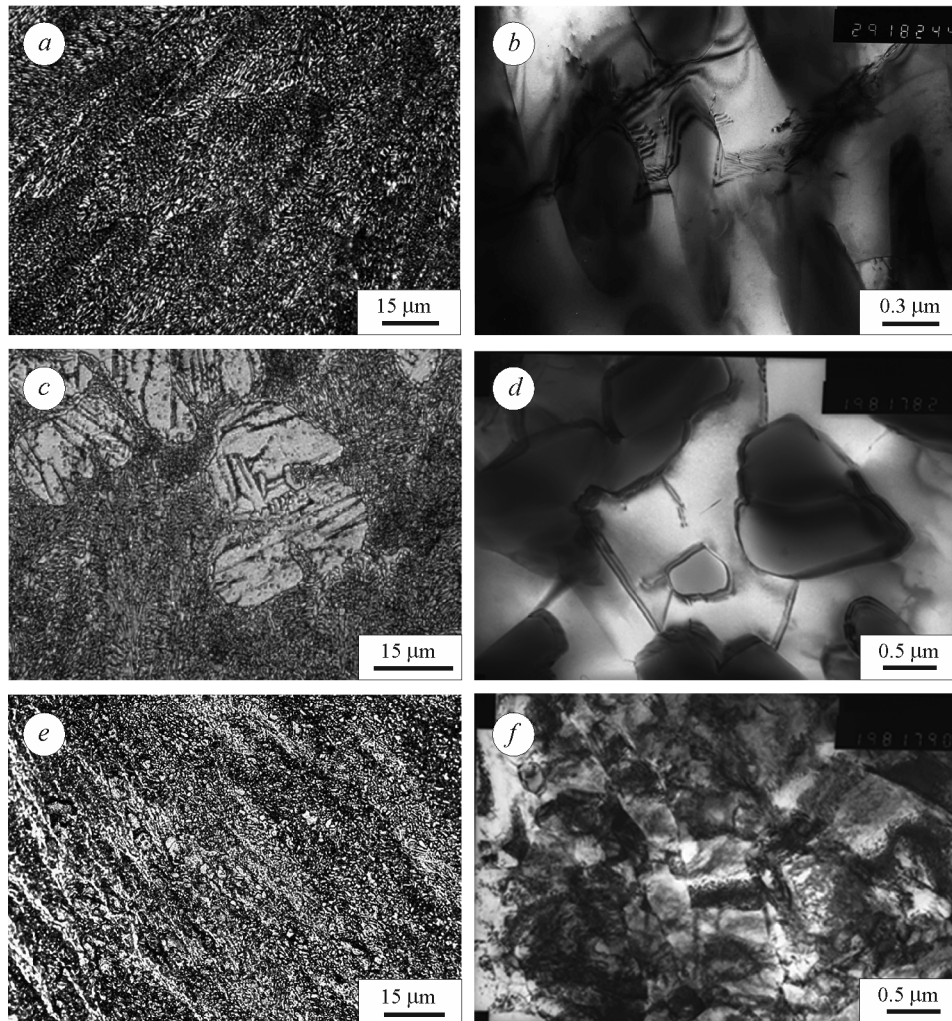


Fig. 1. Structural microphotographs for the cast Ti–10Si–10Zr–1Sn (*a, b*) and Ti–9Si–7.6Zr (*c, d*) alloys and for the thermomechanically treated Ti–9Si–7.6Zr alloy (*e, f*): optical (*a, c, e*) and transmission (*b, d, f*) microscopy [18, 20]

TABLE 2. Tribotechnical Characteristics for the Eutectic Ti–Si–Zr Alloy Samples Determined by Tests Using an M-22M Friction Machine with a ShKh15 Steel Indenter

Alloy	Sliding speed V , m/sec	Friction coefficient f	Linear wear rate for the friction pair I , $\mu\text{m}/\text{km}$	Weight wear rate I , mg/km		Friction force F , N ($F = f \cdot N$)
				Sample	Counterface	
Ti–10Si–10Zr–1Sn (cast)	1	0.7	9.8	7.2	0.7	14
	2	0.6	27	18	0.33	12
	4	0.47	28	21.7	0.23	9.4
	6	0.38	27	28.4	0.23	7.6
Ti–9Si–7.6Zr (cast)	1	0.63	8.3	6.4	1.4	12.6
	2	0.6	16	13.9	1.1	12
	4	0.58	13	12.2	0.5	11.6
	6	0.35	19	20.8	0.2	7

microphotograph of the cast alloy from the eutectic grain area. According to [20], further thermomechanical treatment refines the alloy, including eutectic grain areas, resulting in a cellular deformation structure. This ultra-fine, virtually grain deformation structure with grain sizes varying from several tens of a micrometer to 1 μm is shown in Fig. 1e, f. Note that the phase composition of the alloy following thermomechanical treatment did not change according to X-ray diffraction (Table 1).

Two cast alloy samples, Ti–10Si–10Zr–1Sn and Ti–9Si–7.6Zr, were tested by dry friction against a ShKh15 steel indenter using an M-22M machine. Analysis of tribotechnical characteristics (Table 2) indicates that the friction coefficients of the Ti–10Si–10Zr–1Sn and Ti–9Si–7.6Zr alloys are quite close. Moreover, this characteristic decreases nonlinearly with increasing sliding speed. At a speed of 6 m/sec, the friction coefficient is ~ 0.38 for the Ti–10Si–10Zr–1Sn alloy and ~ 0.35 for the Ti–9Si–7.6Zr alloy. At the same time, the linear and weight wear rates for the cast Ti–10Si–10Zr–1Sn sample at the greatest test speed are 1.4 times higher than those for the Ti–9Si–7.6Zr alloy. Note that the friction coefficients are significantly lower than the values peculiar to titanium alloys in the absence of lubrication (~ 0.6 [1, 2]). For all V values studied, the total linear wear rate for the cast Ti–10Si–10Zr–1Sn alloy is $\sim 91.8 \mu\text{m}/\text{km}$ (average value for the four sliding speeds is $22.95 \mu\text{m}/\text{km}$) and for the cast Ti–9Si–7.6Zr alloy is $56.3 \mu\text{m}/\text{km}$ (average value is $14.08 \mu\text{m}/\text{km}$). The difference is $\sim 60\%$.

Small dark separation film developed on the contact surfaces of the Ti–10Si–10Zr–1Sn sample and the counterface in friction at sliding speeds of 1 and 2 m/sec and disappeared when the sliding speed increased to 6 m/sec. Note that there were individual areas where the sample stuck to the counterface, being indicative of frictional seizure. This was not the case in the friction of the cast Ti–9Si–7.6Zr sample at the same sliding speeds, but dark separation film developed on the counterface without any obvious signs of seizure. Seizure [27] is one of the most undesirable types of surface damage; it is especially intensive at low sliding speeds and significant loads. Hence, in the second series of tests, the tribological behavior of Ti–Si–Zr alloys was studied in more severe conditions under quasistatic and dynamic loads with Si_3N_4 and ShKh15 indenters at a much lower sliding speed than in the first method. The test results for the second method using a computer-assisted tribology system are presented in Table 3. According to this method, the thermomechanically treated Ti–9Si–7.6Zr alloy was studied along with the cast alloys.

The study of wear in two loading modes using steel and ceramic indenters revealed significant differences in the friction of eutectic Ti–Si–Zr alloys.

The antifriction properties of both cast alloys were virtually the same in the first (Table 2) and second (Table 3) test methods, but the friction coefficient for the cast Ti–9Si–7.6Zr alloy was 20% lower than that for the cast Ti–10Si–10Zr–1Sn alloy.

Table 2 shows that the wear rate for the cast hypoeutectic Ti–9Si–7.6Zr alloy determined with the first friction method is 1.4 times lower than the wear rate for the Ti–10Si–10Zr–1Sn alloy with a superfine eutectic structure. Contact load is an important factor that directly influences processes in the contact area [28]. Hence, the

TABLE 3. Tribotechnical Characteristics for the Eutectic Ti–Si–Zr Alloy Samples Determined at Quasistatic and Dynamic Loads Using a Computer-Assisted Tribological System

Alloy, at.%	Indenter material	Linear wear, μm		Friction force, N		Friction coefficient	
		I^{st}	I^{dyn}	F^{st}	F^{dyn}	f_{st}	f_{dyn}
Ti–10Si–10Zr–1Sn (cast)	ShKh15	23.20	18.45	22.25	4.69	0.74	0.16
	Si_3N_4	23.29	15.47	29.76	3.82	0.99	0.13
Ti–9Si–7.6Zr (cast)	Si_3N_4	18.92	13.64	22.55	5.31	0.75	0.18
Ti–9Si–7.6Zr (treated thermomechanically)	ShKh15	4.92	5.89	18.20	1.23	0.29	0.08
	Si_3N_4	11.44	8.33	31.64	5.69	1.05	0.19

Ti–9Si–7.6Zr alloy remained advantageous in terms of wear resistance determined with the second method of friction against Si_3N_4 , but its value was somewhat lower in both loading modes. Dynamic loading led to lower wear than quasistatic loading did (Table 3), in contrast to the data reported previously in [29–31], in particular, for cast irons and steels [26] for which the opposite effect was observed. The wear of eutectic Ti–Si–Zr alloys is lower under dynamic loads and is similar to the wear for some ceramic materials that are also characterized by high friction coefficient (~ 0.7) [32, 33]. This fact is confirmed by studies on the relief of friction paths (Fig. 2). The friction surface of the thermomechanically treated Ti–9Si–7.6Zr alloy sample tested with Si_3N_4 (Fig. 2a, b) has sliding paths with numerous seizure areas, which may be indicative of predominant adhesive friction [10]. When friction changes from quasistatic to dynamic, the surface becomes smoother with noticeable sliding paths (Fig. 2b). The appearance of typical clear sliding paths may result from the participation of hard silicide particles that strengthen the alloy in the wear process. Strong bonding at the silicide–titanium matrix interface is promoted by special conditions for the crystallization of eutectic alloys; this was mentioned previously [12, 13] and confirmed for the Ti–Si alloys in [34, 35].

Under dynamic testing, being characterized by lower friction force than observed in quasistatic loading (Table 3), adhesive wear may change to predominant abrasive wear, and lower wear under dynamic loading is indicative of the features peculiar to the eutectic Ti–Si alloys.

The friction process for the eutectic Ti–Si–Zr alloys also differs by high wear characteristics in use of the Si_3N_4 indenter compared to the ShKh15 indenter, as evidenced by the data reported in Table 3 and by the appearance and width of the friction paths in Fig. 2.

According to the results obtained, the eutectic Ti–10Si–10Zr–1Sn alloy with a superfine structure demonstrates the lowest wear resistance under quasistatic and dynamic loads, regardless of the indenter material (Table 3). Under quasistatic loading, the alloy shows high friction coefficient— $f_{\text{st}} = 0.74$ and 0.99 for ShKh15 and Si_3N_4 indenters—and wear rate is maximum among all the alloys. The best tribotechnical characteristics with the lowest friction coefficients, $f_{\text{st}} = 0.29$ and $f_{\text{dyn}} = 0.08$, and the lowest wear rates, $I_{\text{st}} = 4.92$ and $I_{\text{dyn}} = 5.89$, are shown by the thermomechanically treated Ti–9Si–7.6Zr sample in friction against the ShKh15 indenter. This friction behavior is probably due to changes in the structural state of the thermomechanically treated alloy resulting from the formation of a deformation cellular structure and the refinement of eutectic grains and silicides (Fig. 1f) [34] and from better compatibility with the ShKh15 indenter. With use of the Si_3N_4 indenter, this alloy has a friction coefficient greater than one under quasistatic loading, and friction force $F^{\text{st}} = 31.64$ N exceeds the load ($N = 30$ N). Similarly to [10, 36], this fact may be indicative of seizure or adhesion between the contacting bodies in the quasistatic loading conditions concerned.

The data determined under different friction conditions for the eutectic Ti–Si–Zr alloys (Tables 2 and 3) contradict the generally accepted views according to which a finer structure promotes better tribotechnical properties under the same test conditions [10]. In this case, the eutectic Ti–10Si–10Zr–1Sn alloy has approximately 50 vol.% of the strengthening phase, and the sizes of silicides are very small (~ 0.3 – 1.0 μm). This heterogeneous

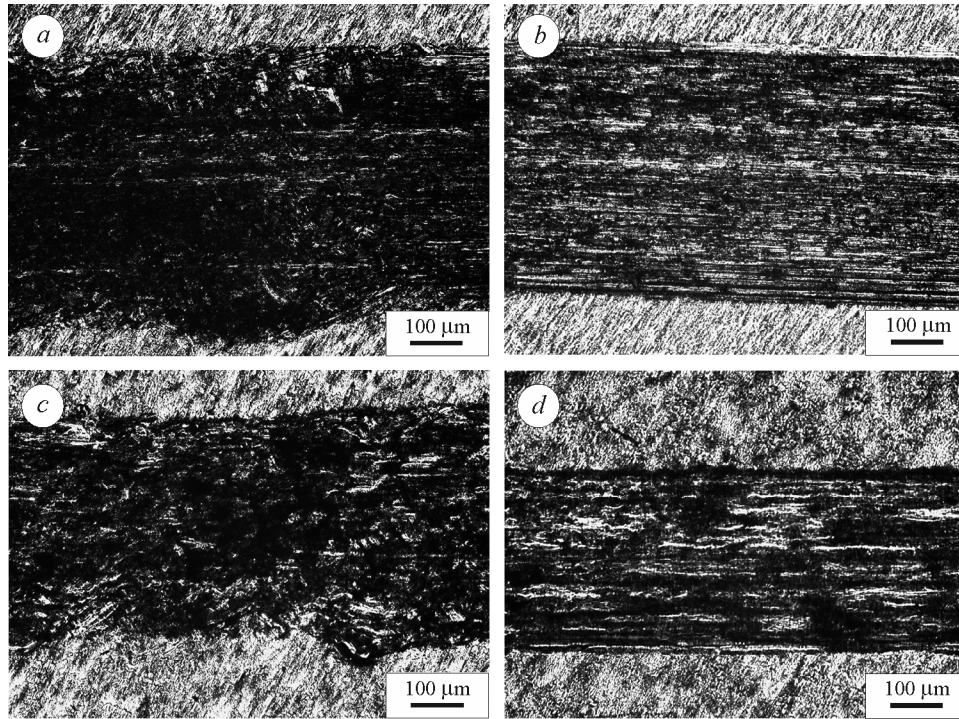


Fig. 2. Microphotographs of friction paths for the Ti–9Si–7.6Zr alloy (treated thermomechanically) with ceramic Si₃N₄ (*a, b*) and steel ShKh15 (*c, d*) indenters: *a, c*) static loading and *b, d*) dynamic loading (optical microscopy)

structure may not comply with the general requirements for wear resistance of the materials, pursuant to which the volume content of the strengthening phase should not exceed ~40% to reach the optimal tribotechnical characteristics [11, 37].

On the other hand, the structural refinement of the thermomechanically treated Ti–9Si–7.6Zr alloy is, as discussed above, one of the influencing factors that contribute to increase in the wear resistance: it became higher by more than 1.65 times compared to the cast alloy.

Change in the counterface material does not always influence the tribotechnical properties of titanium-based alloys [6], which was confirmed by studies of the cast Ti–10Si–10Zr–1Sn alloy (Table 3). However, the noticeable difference in the tribological characteristics of the thermomechanically treated Ti–9Si–7.6Zr alloy tested with steel (ShKh15) and ceramic (Si₃N₄) indenters is indicative of a significant role of the counterface material and confirms the physicochemical interaction between the sample and counterface. Silicon that is present in the ceramic indenter may lead to greater adhesive interaction between the sample and the counterface in friction under quasistatic loading for all samples, especially for the thermomechanically treated Ti–9Si–7.6Zr alloy, which intensifies wear processes and significantly increases the friction force.

Thus, reduction in the effect of adhesive friction—both through changes in the loading and indenter material and in the refinement of silicides—results in transition to ‘normal’ mechanochemical wear [38], which is characterized by small wear and low friction coefficient (Table 3). Better wear resistance and compatibility are promoted by the thermomechanically treated Ti–9Si–7.6Zr alloy in friction against ShKh15 under quasistatic and dynamic loading.

CONCLUSIONS

The wear of cast *in situ* Ti–Si–Zr composites with high zirconium content was studied in different conditions of friction against ShKh15 steel. The hypoeutectic Ti–9Si–7.6Zr alloy showed improved tribotechnical properties compared to the eutectic Ti–10Si–10Zr–1Sn alloy characterized by a heterogeneous superfine structure.

The wear resistance of the Ti–9Si–7.6Zr alloy was found to be almost 60% higher than that of the cast Ti–10Si–10Zr–1Sn alloy; i.e., the linear wear rate of the cast Ti–10Si–10Zr–1Sn alloy was higher than that of the Ti–9Si–7.6Zr alloy.

Contrastingly to conventional tribotechnical materials (cast irons and steels), the wear resistance of eutectic Ti–Si–Zr alloys was shown for the first time to increase when loading changed from quasistatic to dynamic. In this case, when the friction coefficient was artificially reduced under dynamic loading conditions, the wear mechanism changed from predominant adhesive to predominant abrasive. Hence, the behavior of such alloys under dynamic loading resembles the behavior of some ceramic materials, being characterized by high friction coefficient as well (~0.7).

The noticeable difference in the tribological characteristics of the thermomechanically treated Ti–9Si–7.6Zr alloy determined in friction against steel (ShKh15) and ceramic (Si₃N₄) indenters is indicative of physicochemical interaction between the sample and counterface and confirms that the counterface material is significant for the friction of heterogeneous Ti–Si–Zr alloys with an e(β^* -Ti + (Ti, Zr)₂Si) eutectic. Better wear resistance and compatibility of the titanium alloy are observed in friction against ShKh15.

The thermomechanical treatment of the cast hypoeutectic Ti–9Si–7.6Zr alloy (rolling at 1000°C to 66% reduction) increases its wear resistance compared to the cast alloy by more than 60%. Thermomechanical treatment refines the structure, including eutectic grains and silicide phase, and results in a superfine, virtually grain deformation structure. This, in turn, is one of the factors that promote transition from predominant adhesive and abrasive wear to normal mechanochemical wear in test conditions.

REFERENCES

1. S.G. Glazunov and V.N. Moiseev, *Titanium Alloys. Structural Titanium Alloys* [in Russian], Metallurgiya, Moscow (1974), p. 308.
2. I.V. Gorynin and B.B. Chechulin, *Titanium Alloys in Mechanical Engineering* [in Russian], Mashinostroenie, Moscow (1990), p. 400.
3. B.K. Vulf, *Heat Treatment of Titanium Alloys* [in Russian], Metallurgiya, Moscow (1969), p. 376.
4. Marc Long and H.J. Rack, “Friction and surface behavior of selected titanium alloys during reciprocating-sliding motion,” *Wear*, **249**, 158–168 (2001).
5. S.V. Putyrsky, A.A. Arislanov, N.I. Artemenko, and A.L. Yakovlev, “Different methods for increasing the wear resistance of titanium alloys and comparative analysis of their effectiveness with respect to the VT23M titanium alloy,” *Aviat. Mater. Tekhnol.*, **50**, No. 1, 19–24 (2018), <https://doi.org/10.18577/2071-9240-2018-0-1-19-24>.
6. A.P. Kudrin, V.V. Zhiginas, V.F. Labunets, and Yu.B. Burbrela, “Effect of laser strengthening on the tribotechnical characteristics of the VT6 titanium alloy,” *Probl. Tert. Znosh.*, No. 52, 152–161 (2009), <https://doi.org/10.18372/0370-2197.52.3126>.
7. I.A. Kazantsev, A.O. Krivenko, A.E. Rozen, and S.N. Chugunov, “Wear resistance of titanium-based composites produced by microarc oxidation,” *Izv. Vuz.*, No. 1, 159–164 (2008).
8. M.Yu. Smolyakova and D.S. Vershinin, “Studying the tribological characteristics of layers modified with nitrogen ions on the VT16 titanium alloy,” *Vest. TGTU*, **18**, No. 4, 1062–1066 (2012).
9. V.P. Prilytskii, S.B. Rukhanovskii, S.V. Akhonin, N.F. Gadzyra, and N.K. Davidchuk, “Increase in the wear resistance of titanium using argon arc deposition,” *Avtomat. Svarka*, **705**, No. 1, 18–20 (2012).
10. B.I. Kostetski, “Structural energy adaptability of materials in friction,” *Tren. Iznos*, **6**, No. 2, 202–212 (1985).
11. N.K. Myshkin and M.I. Petrokovets, *Friction, Lubrication, and Wear. Physical Fundamentals and Technical Applications of Tribology* [in Russian], Fizmatlit, Moscow (2007), p. 368.
12. A.I. Somov and M.A. Tikhonovskii, *Eutectic Composites* [in Russian], Metallurgiya, Moscow (1975), p. 304, [https://doi.org/10.1016/0007-117X\(75\)90065-7](https://doi.org/10.1016/0007-117X(75)90065-7).

13. Yu.N. Taran and V.I. Mazur, *Structure of Eutectic Alloys* [in Russian], Metallurgiya, Moscow (1978), p. 330.
14. S.A. Firstov, S.V. Tkachenko, and N.N. Kuzmenko, "Titanium pigs and titanium steels," *Metalloved. Term. Obrab. Met.*, **643**, No. 1, 14–20 (2009).
15. Yu.N. Taran, V.I. Mazur, S.V. Kapustnikova, S.A. Firstov, and L.D. Kulak, "New metal ceramic titanium-based materials," *Met. Lit. Ukrainy*, No. 11–12, 42–46 (1999).
16. S. Firstov, "The main tendencies in elaboration of materials with high specific strength," *Met. Mater. Struct. Eff. Proc. NATO. NATO Sci. Ser. II. Math. Phys. Chem.*, **146**, 33–44 (2004), https://doi.org/10.1007/1-4020-2112-7_3.
17. M.V. Bulanova, I.D. Gornaya, K.A. Meleshevich, V.A. Saltykov, A.V. Samelyuk, L.A. Tretiachenko, and S.A. Firstov, "Structure and properties of cast Ti–Zr–Si alloys," *Dop. Nats. Akad. Nauk Ukrainy*, No. 4, 86–90 (2004).
18. I.D. Gorna, K.O. Gorpenko, O.Yu. Koval, A.V. Kotko, and S.O. Firstov, "Structure and mechanical properties of Ti–Si–X alloys," *Fiz. Khim. Mekh. Mater.*, No. 3, 35–42 (2008).
19. I. Gornaya, O. Bankovsky, N. Bega, L. Kulak, D. Miracle, and S. Firstov, "Effect of Zr on structure and mechanical properties of Ti–Al–Si alloys," *Met. Mater. Struct. Eff. Proc. NATO. NATO Sci. Ser. II. Math. Phys. Chem.*, **146**, 229–234 (2004), <https://doi.org/10.1007/1-4020-2112-723>.
20. K.O. Valuyskaya, "Structural and mechanical properties of Ti–Si–X alloys with additional intermetallic strengthening," *Author's Abstract of PhD Thesis in Technical Sciences* [in Ukrainian], 05.16.01, Kyiv (2012), p. 27.
21. S. Tkachenko, O. Datskevich, L. Kulak, and H. Engqvist, "Tribological properties of Ti–Si–Zr alloys," in: *Proc. 22nd Conf. Metall. Mater. METAL* (2013), pp. 15–17.
22. Yongzhong Zhan, Zhengwen Yu, Ying Wang, Yanfei Xu, and Xiabo Shi, "Microstructure and tribological behavior of Ti–Si eutectic alloys with Al addition," *Tribol. Lett.*, **26**, No. 1, 25–31 (2007), <https://doi.org/10.1007/s11249-006-9178-5>.
23. K.O. Valuyskaya, I.D. Gorna, V.T. Varchenko, M.D. Bega, I.Yu. Okun, Ya.I. Evich, and S.O. Firstov, "Wear resistance of *in situ* Ti–Si–Ga composites," *Elektron. Mikrosk. Prochn. Mater.*, No. 24, 47–53 (2018), <http://www.materials.kiev.ua/publications/EMMM/2018/7.pdf>.
24. A.A. Adamovskii, V.M. Emtsov, and V.T. Varchenko, "Methodology for studying the tribotechnical characteristics of superhard materials based on dense boron nitride modifications," *Adhez. Raspl. Paika Mater.*, No. 42, 77–84 (2009).
25. N.A. Zenkin and K.E. Grinkevich, "Diagnostic equipment and methodology for monitoring of tribological system parameters in dynamic testing conditions," *Kontr. Diagn.*, No. 6, 49–51 (2002).
26. J. Wang, H. Li, and K. Grinkevych, "Cyclic indentation method applied to evaluating surface degradation of cylinder-piston group parts," *Strength Mater.*, 775–783 (2021), <https://doi.org/10.1007/s11223-021-00343-6>.
27. A.I. Dotsenko and I.A. Buyanovskii, *Fundamentals of Tribological Engineering* [in Russian], INFRA-M, Moscow (2014), p. 336.
28. D.H. Buckley, *Surface Effects in Adhesion and Friction* [Russian translation], Mashinostroenie, Moscow (1986), p. 359.
29. K.E. Grinkevich, "Some provisions of the structural and dynamic tribological system concept and their implementation," *Tren. Iznos*, **24**, No. 3, 344–350 (2003).
30. E. Roman, K.E. Grinkevych, and I. Martínez, "TriDes—a new tool for the design, development and non-destructive evaluation of advanced construction steels," *Mater. Constr.*, **66**, No. 324, e099 (2016).
31. Yu.V. Milman, G.M. Nikiforchin, K.E. Grinkevich, O.T. Tsyurulnik, I.V. Tkachenko, V.A. Voloshyn, and L.V. Mordel, "Assessing operational degradation of gas piping steel by destructive and nondestructive methods," *Fiz. Khim. Mekh. Mater.*, **47**, No. 5, 13–18 (2011).

32. O. Zgalat-Lozynskyy, N. Tischenko, and O. Shirokov, "Deformation treatment in spark plasma sintering equipment and properties of AlON-based ceramic," *J. Mater. Eng. Perform.*, **31**, No. 3, 2575–2582 (2021), <https://doi.org/10.1007/s11665-021-06381-0>.
33. O.B. Zgalat-Lozynskyy, L.I. Ieremenko, I.V. Tkachenko, K.E. Grinkevich, S.E. Ivanchenko, A.V. Zelinskiy, G.V. Shpakova, and A.V. Ragulya, "Tribological properties of ZrN–Si₃N₄–TiN composites consolidated by spark plasma sintering," *Powder Metall. Met. Ceram.*, **60**, 597–607 (2022), <https://doi.org/10.1007/s11106-022-00272-2>.
34. S.O. Firstov, "New generation of titanium-based materials," *Fracture Mechanics of Materials and Structural Strength* [in Ukrainian] (2004), pp. 609–616.
35. M.M. Kuzmenko, "Effect of plastic deformation on the structure and mechanical properties of Ti–Si alloys," *Sovr. Probl. Fiz. Materialoved.*, No. 16, 118–121 (2007), <http://www.materials.kiev.ua/issue/3/article/163>.
36. A.A.C. Recco, I.C. Oliveira, M. Massi, H.S. Maciel, and A.P. Tschiptschin, "Adhesion of reactive magnetron sputtered TiN_x and TiC_y coatings to AISI H13 tool steel," *Surf. Coat. Technol.*, **202**, 1078–1083 (2007).
37. O. Zgalat-Lozynskyy, I. Kud, L. Ieremenko, L. Krushynska, D. Zyatkevych, K. Grinkevych, O. Myslyvchenko, V. Danylenko, S. Sokhan, and A. Ragulya, "Synthesis and spark plasma sintering of Si₃N₄–ZrN self-healing composites," *J. Eur. Ceram. Soc.*, **42**, No. 7, 3192–3203 (2022), <https://doi.org/10.1016/j.jeurceramsoc.2022.02.033>.
38. V. Pinchuk and S. Korotkevich, *Strengthening Kinetics and Fracture of the Surface Metal Layer in Friction* [in Russian], LAP, Saarbrücken (2013), p. 180.